Chemical Engineering Science 63 (2008) 5314 – 5329

Contents lists available at ScienceDirect

Chemical Engineering Science

journal homepage: www.elsevier.com/locate/ces

# Countermeasures against alkali-related problems during combustion of biomass in a circulating fluidized bed boiler

K.O. Davidsson[a,*], L.-E. Åmand[a], B.-M. Steenari[b], A.-L. Elled[a], D. Eskilsson[c], B. Leckner[a]

[a]Department of Energy and Environment, Chalmers University of Technology, SE-412 96 Göteborg, Sweden
[b]Department of Chemical and Biological Engineering, Chalmers University of Technology, SE-412 96 Göteborg, Sweden
[c]SP Technical Research Institute of Sweden, Box 857, SE-501 15 Borås, Sweden

ARTICLE INFO

*Article history:*
Received 28 March 2008
Received in revised form 10 June 2008
Accepted 1 July 2008
Available online 15 July 2008

*Keywords:*
Agglomeration
Biofuels
Combustion
Deposition
Gases
Particulate processes

ABSTRACT

The purpose of this work was to study different ways to mitigate alkali-related problems during combustion of biomass in circulating fluidized beds. Wood chips and wood pellets were fired together with straw pellets, while the tendency to agglomerate and form deposits was monitored. In addition to a reference case, a number of countermeasures were applied in related tests. Those were addition of elemental sulphur, ammonium sulphate and kaolin to a bed of silica sand, as well as use of olivine sand and blast-furnace slag as alternative bed materials. The agglomeration temperature, composition and structure of bed-ash samples were examined. The flue-gas composition, including gaseous alkali chlorides, was measured in the hot flue gases and in the stack. Particles in the flue gas were collected and analysed for size distribution and composition. Deposits were collected on a probe in hot flue gases and their amount and composition were analysed. Addition of kaolin was found to be the best method to counteract the agglomeration problem. The deposition problem is effectively counteracted with addition of ammonium sulphate, while kaolin is too expensive to be used commercially against deposits, and sulphur is less effective than ammonium sulphate.



## 1. Introduction

The combustion of biomass in fluidized beds may cause operational problems such as agglomeration of the bed material and deposits on superheater tubes. In both these problems alkali is involved (Ergudenler and Gahly, 1993; Miles et al., 1996; Nielsen et al., 2000). The alkali is released from the fuel during conversion. It may thereafter be transported to the surface of the bed particles forming a sticky layer, which favours agglomeration (Öhman et al., 2000). This is often the case when the usual silica-rich sand is used as bed material, since alkali silicates with low melting points are formed. In severe cases, defluidization occurs. The released alkali can also be carried away by the flue gas as particles or in gaseous form, e.g. as chlorides. When it reaches the relatively cold surface of superheater tubes, condensation of gaseous alkali species and deposition of particles may occur, forming a layer on the tubes (Baxter et al., 1998; Westberg et al., 2003). The deposit reduces heat transfer and, depending on composition, favours further deposition and corrosion. To shut the plant down in order to remove agglomerates or deposits, or having to replace super-heater tubes, is costly. Therefore various countermeasures to prevent these problems have been published.

The countermeasures are choice of fuel, fuel preparation, co-firing with favourable fuels, dosage of certain additives, and alternative bed materials. An effective choice of fuel would be to simply avoid short-rotation crops, such as straw, and fast-growing parts of plants like leaves and twigs, because they contain significant amounts of alkali (Werkelin et al., 2005) and are likely to induce the problems mentioned above. If these fuels cannot be avoided, leaching in water is an efficient fuel preparation, which removes the alkali substances before conversion (Davidsson et al., 2002). If the alkali cannot be removed, it may be chemically altered, so that it is transferred to a less hostile form. This can be achieved by co-firing with a fuel that contains sulphur or aluminium silicates. For example, co-firing with coal or sludge (Davidsson et al., 2007b) or peat (Theis et al., 2006) has been shown to decrease the concentration of alkali chlorides in the flue gas. Sulphur reacts with alkali and forms sulphates (Iisa et al., 1999), which are preferable from a deposition/corrosion point of view. Aluminium silicates react with alkali and form compounds with higher melting points than those in most fluidized bed combustion situations, whereby it prevents agglomeration. Sulphur and aluminium silicates can also be supplied as additives directly to the furnace or the flue-gas channel. Kaolin, which is an aluminium

* Corresponding author. Tel.: +46 31 772 14 53.
*E-mail address:* keda@chalmers.se (K.O. Davidsson).

0009-2509/$ - see front matter © 2008 Elsevier Ltd. All rights reserved.
doi:10.1016/j.ces.2008.07.012

silicate, has been shown to increase the melting point of the bed material in fluidized bed combustion (Davidsson et al., 2007a). Addition of sulphur to the furnace and addition of ammonium sulphate to the cyclone shifts alkali from chlorides to sulphates (Kassman et al., 2006). The sulphation reaction is fast in the gas phase, and occurs between the alkali chloride and $SO_3$ (Iisa et al., 1999). The rate-limiting step is the formation of $SO_3$ (Iisa et al., 1999), which is formed from $SO_2$ or $SO_4^{2-}$; $SO_2$ being the product of oxidation of sulphur, and $SO_4^{2-}$ being the product of dissociation of the ammonium sulphate. Alternative bed materials are such that contain little quartz to prevent the formation of alkali silicates. Examples of alternative materials are olivine and blast-furnace slag (Brus et al., 2004).

The various counter-measures mentioned here are usually aimed at solving either the agglomeration or the deposition problem. However, preventing one of the problems can affect the other. For instance, the use of a bed material that does not react with alkali may result in a higher concentration of alkali chlorides in the flue gas and thereby cause more deposits. Another example is the addition of sulphur to the furnace in order to lower the alkali chloride concentration in the flue gas. This may also affect the agglomeration tendency of the bed. Addition of kaolin may have the result that alkali is bound in the bed and less is available for the gaseous phase. This should lead to less deposition. Because the counter-measures may affect both the bed agglomeration and the deposition tendency, they should be followed simultaneously.

In the mechanisms involved when using additives or alternative bed materials, not only the chemical mechanisms but also the retention time are important. This is especially important in reactions between solid and gaseous substances. To achieve retention times characteristic for a large-scale conversion, the present experiments were performed in a full-scale test facility (12 $MW_{th}$ circulating fluidized bed boiler). In a previous study in the same facility, biomass, coal and sludge were co-fired in order to minimize deposition (Davidsson et al., 2007b). In the present study, the addition of elemental sulphur, sulphate, and kaolin and the use of different bed materials were investigated during firing of biomass of high alkali content. The effect on bed agglomeration and deposition were studied simultaneously. Different dosages were applied. This means that not only the effect of a certain additive is established, but also how much needs to be added. Furthermore, cost assessments are made in order to judge whether a suggested countermeasure is economical; i.e. if the cost is less than the expected cost resulting from bed agglomeration or deposits. To summarize, the major purposes of the present study are

- to quantify the effect of certain alkali-related countermeasures on both bed agglomeration and superheater deposits;
- to assess the costs associated with the countermeasures.

## 2. Experiments

### 2.1. Fuels

Table 1 shows the composition of the fuels. The most important difference between wood and straw pellets is that straw pellets has a much higher chlorine content and ash fraction. The high ash fraction implies a considerably higher content of alkali. The straw pellets are used for controlling the alkali load in the experiments.

### 2.2. The boiler

The boiler is shown schematically in Fig. 1. The furnace has a quadratic cross-section of 2.25 $m^2$ and a height of 13.4 m. The flue gases and the bed material are separated in the cyclone. Before the convection pass, the flue gases are about 800 °C. At this spot, gas sampling takes place and the alkali chlorides are measured in situ. The flue gas is cooled to about 150 °C in the convection pass and the economizer. Gas analysis also takes place before and after the fly ash separators (secondary cyclone and bag filters).

The boiler was operated according to the parameters in Table 2, as a circulating fluidized bed.

**Table 1**
Composition of fuels

| | Straw pellets | Wood pellets |
|---|---|---|
| *Proximate analysis* | | |
| Moisture (wt% as received) | 8.8 | 8.0 |
| Ash (wt% dry) | 5.6 | 0.3 |
| Combustible (wt% dry) | 94.4 | 99.7 |
| Volatile (wt% daf) | 81.1 | 82 |
| *Ultimate analysis (wt% daf)* | | |
| C | 49.4 | 50.5 |
| H | 6.3 | 6.1 |
| O | 43.4 | 43.3 |
| S | 0.10 | <0.01 |
| N | 0.59 | 0.06 |
| Cl | 0.30 | <0.01 |
| *Ash analysis (g/kg dry ash)* | | |
| K | 110 | 97.4 |
| Na | 9.0 | 9 |
| Al | 6.5 | 8 |
| Si | 300 | 40.9 |
| Fe | 2.1 | 8.4 |
| Ca | 52 | 212 |
| Mg | 10 | 33.8 |
| P | 14 | 11.7 |
| Ti | 0.4 | 1.1 |
| Ba | 0.4 | 3.7 |
| *Heating value (MJ/kg)* | | |
| H, daf | 18.4 | 18.9 |
| H, as received | 15.6 | 17.1 |

daf, dry and ash free.

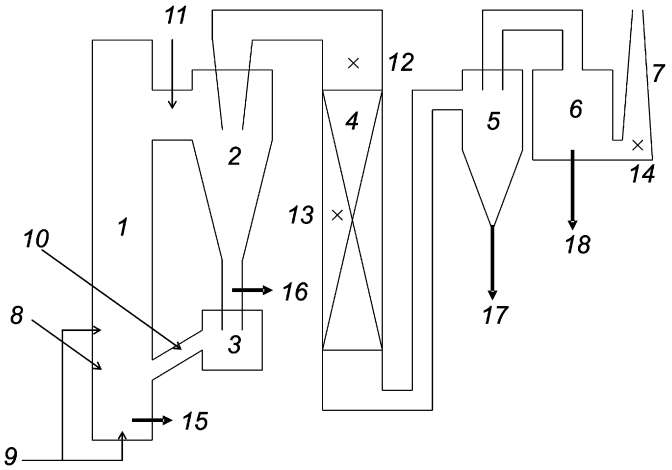


**Fig. 1.** Schematic picture of the 12 MW circulating fluidized bed at Chalmers. 1, furnace; 2, cyclone; 3, particle seal; 4, convection pass; 5, secondary cyclone; 6, bag filter; 7, stack; 8, fuel feed/bed material; 9, air; 10, sulphur granules/kaolin; 11, ammonium sulphate; 12, gas measurement position before convection pass, and deposit probe; 13, measurement position for particles (impactor); 14, gas measurement position for stack; 15, bed ash; 16, cyclone-leg ash; 17, secondary cyclone ash; 18, bag filter ash.

### 2.3. Procedure

Table 3 shows the names and characteristics of the individual experiments. The names consist of letters, which indicate the most

important feature of the experiment. For instance, the reference cases are called $ref_1$ and $ref_2$; the numbers denote different experiments with the same operational parameters. Other numbers indicate the amount of additive. Normally the experiments lasted for 12 h. Some of the experiments were extended to allow for possible transients to disappear. These long-term experiments are denoted by an *L*. It was found that 12 h was enough to assure steady-state conditions for most items investigated. Olivine sand was introduced after the silica sand was removed with the boiler shut down. The blast-furnace slag was continuously fed to the furnace for a week in order to thoroughly replace the silica sand. A 12 h experiment started after at least 12 h of firing with wood pellets only and normal bed regeneration. Before the start of an experiment, bottom and fly ash samples were collected and thereafter the operating parameters were set. At the start of an experiment, i.e. at 0 h, additional fuels (straw pellets and possibly sewage sludge) and additives were supplied. Bed-ash samples were taken at 4 and 8 h. At 6 h the deposit probe was inserted and gas measurements were performed until the end of the experiment. Before ending the experiments at 12 h, bottom and fly ash samples were taken. A long-term experiment starts directly after a corresponding 12 h experiment by shutting off the forced bed ejection, allowing ejection only to keep the pressure drop over the bed constant. During the long-term experiment the deposit probe was inserted for longer periods than 4 h. Gas measurements and ash sampling were performed over the entire period, which may be 20–60 h.

**Table 2**
Operating parameters

| Parameter | Average | Standard deviation |
|---|---|---|
| Thermal load (MW) | 6.2 | 0.24 |
| Wood pellets (kg ds/h)[a] | 1048 | 31 |
| Straw pellets (kg ds/h)[a] | 276 | 4 |
| Fraction of straw pellets (% of load) | 20 | 0.8 |
| Bed temperature top (°C) | 851 | 2 |
| Bed temperature bottom (°C) | 870 | 5 |
| Cyclone outlet temperature (°C) | 822 | 10 |
| Flue-gas temperature after bag filter (°C) | 153 | 1 |
| Pressure drop in furnace (kPa) | 7.3 | 0.3 |
| Excess air ratio | 1.19 | 0.02 |
| Primary air/secondary air (%) | 51 | 5 |
| Fluidization velocity (m/s) | 4.5 | 0.3 |
| Bed turnover high (kg/h) | 83 | 22 |
| Bed turnover high (kg/MW h) | 13 | 4 |

[a]ds, dry substance.

### 2.4. Additives and bed materials

Input flows of additives and bed materials are given in Table 3.

A solution of 40 wt% ammonium sulphate was sprayed into the flue-gas channel (#11 in Fig. 1). The flow was adjusted to a molar ratio S/Cl of approximately 2, 3 or 5 in three experiments. This may not be the most effective position to supply ammonium sulphate to get an effect on the bed material. However, the major purpose of adding ammonium sulphate is to lower gaseous KCl and hazardous deposits on superheater tubes. Therefore, in practice, the chosen position is reasonable.

Elemental sulphur in the form of granules, delivered by JAKOKEM AB, was supplied through the lime supply system (#10 in Fig. 1) to the return leg between the particle seal and the furnace, assuring that the effect of sulphur on the bed would be as high as possible.

Kaolin, under the product name of Intrafill C (RLO 7333), was delivered by Imerys Mineral AB. It was in the form of a fine powder (36% of the particles < 1 μm and 55% of the particles < 2 μm). The kaolin was supplied to the furnace through the lime supply system in order to maximize the effect on the bed.

Olivine sand was used as an alternative bed material. It was delivered by North Cape Minerals (Norway). Its major constituent is $(Mg, Fe)_2SiO_4$.

Blast-furnace slag served as an alterative bed material. It was delivered by SSAB Merox AB. The major constituents are calcium/magnesium/aluminium silicates; a by-product from the production of iron in a blast furnace where iron ore, coke and limestone and olivine are mixed at a high temperature under reducing conditions. The slag exits the blast furnace at a temperature of 1500 °C and is then cooled rapidly forming amorphous blast-furnace slag.

**Table 3**
Experiments and experimental parameters

| Experiment | Duration (h) | Bed material | Additive | Alkali input (mol/h) | S input (mol/h) | Molar input ratios | | Bed turnover (kg/h) |
|---|---|---|---|---|---|---|---|---|
| | | | | | | S/Cl | Kaolin/alkali[a] | |
| *12 h experiments* | | | | | | | | |
| $ref_1$ | 12 | [b] | – | 63 | 13 | 0.47 | 0 | 90 |
| $ref_2$ | 12 | [b] | – | 64 | 10 | 0.50 | 0 | 89 |
| am2 | 12 | [b] | $(NH_4)_2SO_4$ | 66 | 42 | 2.1 | 0 | 86 |
| am3 | 12 | [b] | $(NH_4)_2SO_4$ | 66 | 92 | 3.2 | 0 | 75 |
| am5 | 12 | [b] | $(NH_4)_2SO_4$ | 64 | 140 | 5.1 | 0 | 70 |
| S2 | 12 | [b] | Sulphur | 65 | 42 | 2.0 | 0 | 85 |
| S6 | 12 | [b] | Sulphur | 64 | 130 | 6.4 | 0 | 69 |
| kao2 | 12 | [b] | Kaolin | 64 | 13 | 0.47 | 1.8 | 82 |
| kao5 | 12 | [b] | Kaolin | 64 | 13 | 0.6 | 5.5 | 79 |
| kao10 | 12 | [b] | Kaolin | 65 | 13 | 0.6 | 9.8 | 68 |
| oli | 12 | Olivine | – | 64 | 10 | 0.51 | 0 | 77 |
| bfs | 12 | bfs | – | 66 | 11 | 0.51 | 0 | 149 |
| *Long-term experiments* | | | | | | | | |
| refL | 40 | [b] | | 65 | 10 | 0.50 | | 0 |
| S2L | 21 | [b] | Sulphur | 65 | 38 | 1.9 | | 0 |
| S6L | 23 | [b] | Sulphur | 65 | 130 | 6.3 | | 0 |
| kao2L | 57 | [b] | Kaolin | 65 | 10 | 0.51 | 2.2 | 0 |
| kao5L | 37 | [b] | Kaolin | 64 | 10 | 0.51 | 5.2 | 0 |
| oliL | 57 | Olivine | | 64 | 10 | 0.51 | | 0 |
| bfsL | 60 | bfs | | 65 | 10 | 0.5 | | 13 |

[a]Molar input ratio/stoichiometric ratio.
[b]Quartz-based natural sand.

### 2.5. Analysis methods

The agglomeration temperatures of bed-ash samples were analysed in a special furnace in which a bed material sample of 0.180 kg is inserted in the furnace and fluidized while the temperature is increased. The pressure drop across the fluidized material is monitored. Agglomeration occurs when the material melts and the pressure drop decreases. The temperature at this instant is taken as the agglomeration temperature. This temperature is somewhat device-specific and should not be taken as a material constant. Here it is used for comparison between different experiments.

The cross-section of bed material particles was analysed. The particles were cast in epoxy and cut. The surface was polished and then analysed with SEM-EDX. The instrument was an Electro-scan 2020 linked to an eX1 EDX-system (ESEM). The analysis shows the distribution of elements in the cross-section of the particles.

Ashes were analysed for elements by the accredited laboratory at the SP Technical Research Institute of Sweden.

Flue gas, sampled in two positions (#12 and 14 in Fig. 1), was analysed by standard instruments for $CO_2$, CO, NO$x$, $N_2O$, $SO_2$ and total hydrocarbons, and a fourier transform infra-red (FTIR) instrument, mainly for HCl and $SO_2$. Upstream of the convection pass (#12 in Fig. 1) an In situ Alkali Chloride Monitor (IACM) was positioned. It measures the sum of gaseous alkali chlorides by ultra violet absorption.

Deposits were collected on two steel rings (outer diameter 38 mm) upstream of the convection pass (#12 in Fig. 1) with the flue-gas flow normal to the longitudinal axis of the rings. The rings were fitted on an air-cooled probe, and kept at a surface temperature of 500 °C. Weighing of the rings took place before and after exposition to the flue gas. The composition of the deposit on the ring, made of the material Sandvik Sanicro 28 (main constituents: 34.8 wt% Fe, 31 wt% Ni, 27 wt% Cr) was analysed by the accredited laboratory at the SP Technical Research Institute of Sweden. The deposits on the other ring, made of alloy 304L (main constituents: 68 wt% Fe, 10.2 wt% Ni, 18.5 wt% Cr), were analysed with SEM-EDX.

## 3. Results

### 3.1. Balances

Ash balances were calculated in some of the experiments and expressed as inflow/outflow. The inflow is ash according to the fuel analyses multiplied by the fuel flow. The outflow is the sum of the bottom and fly ash flows. The average of the ash balances in reference and olivine cases ($ref_1$, $ref_2$ and oli) was $1.01 \pm 0.04$; hence, a good closure was obtained. No ash balances were calculated in the other experiments, because they were disrupted by additives and their chemical reactions.

### 3.2. Bottom ash composition

Samples taken from the bed and from the cyclone leg are representative of the bottom ash. These are denoted with the experiment name (Table 3) followed by B or CL, and the number of hours passed since the experiment started (at 0 h). To make the diagrams (Figs. 2–6) clearer, silicon has been omitted in most cases, together with oxygen and carbon, which were not analysed.

Fig. 2 shows the composition of bottom ash in the reference cases. Because the bed sand is quartz-based, silicon dominates the composition in all samples. Calcium and potassium are present at the start of the experiment. The fraction of potassium increases with time in the long-term experiments. Other elements are present in very small amounts.

Fig. 3 shows the composition of bottom ash during addition of kaolin. There is an accumulation of aluminium, potassium and calcium with time. The fraction of magnesium increases significantly in the longest experiments but is not observed in the 12 h experiment.

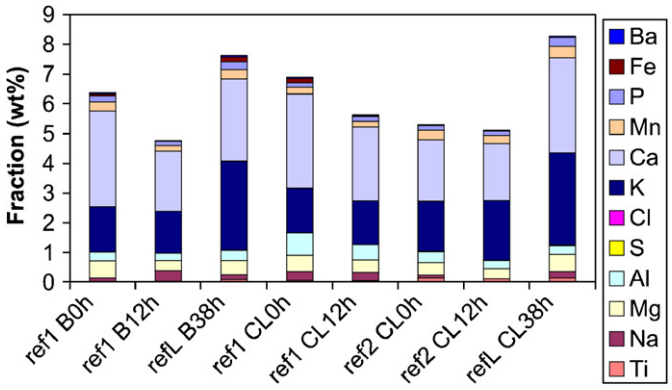


**Fig. 2.** The composition of bottom ash in the reference experiments. Silicon, oxygen and carbon are not included.

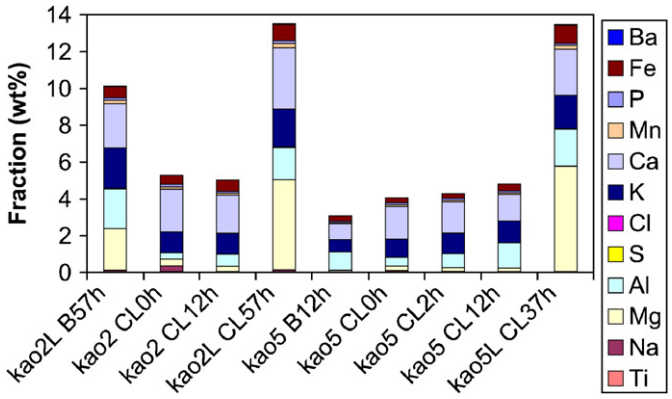


**Fig. 3.** The composition of bottom ash in the experiments with kaolin addition. Silicon, oxygen and carbon are not included.

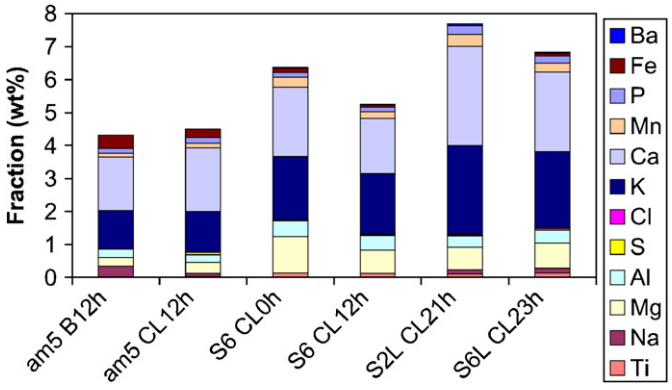


**Fig. 4.** The composition of bottom ash in the experiments with addition of ammonium sulphate and sulphur. Silicon, oxygen and carbon are not included.

Fig. 4 shows the composition of bottom ash in the experiments with addition of ammonium sulphate and sulphur. These additives do not lead to accumulation of sulphur in the bottom ash. The amounts of alkali in the am5 B12h and am5 CL12h are lower than in the corresponding reference samples, but alkali is accumulated in the S6L.

Fig. 5 shows the composition of bottom ash in the experiments where the quartz-based bed sand was replaced by olivine sand,

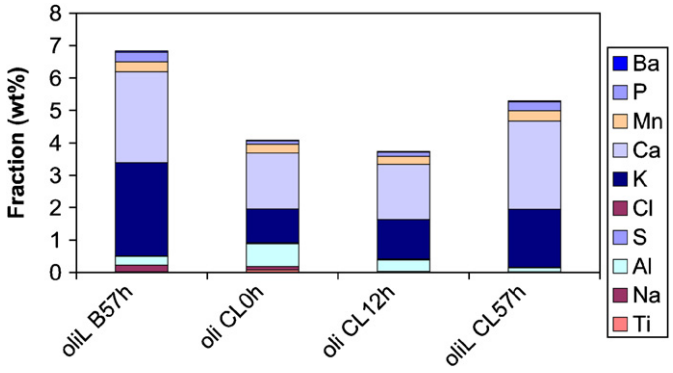


**Fig. 5.** The composition of bottom ash in the experiments with olivine sand. Silicon, iron, magnesium, oxygen and carbon are not included.

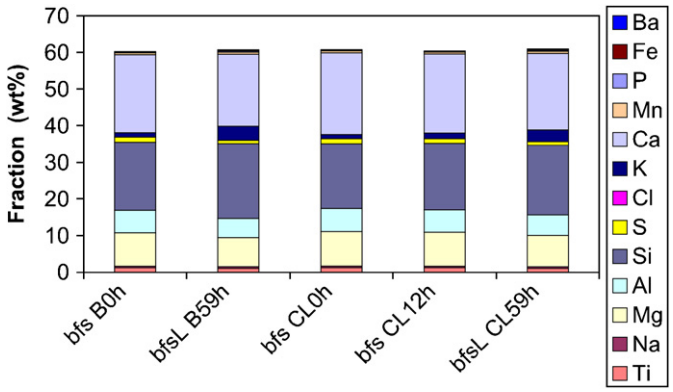


**Fig. 6.** The composition of bottom ash in the experiments with blast furnace slag. Oxygen and carbon are not included.

which is a magnesium/iron silicate. Consequently, the composition is dominated by these elements. The fractions of potassium and calcium increase with time.

Fig. 6 shows the composition of bottom ash in the experiments, where the quartz-based sand was replaced by blast-furnace slag, which contains magnesium/calcium/aluminium silicates. Consequently, the composition is dominated by these elements. Potassium is accumulated with time.

Fig. 7 shows the fraction of alkali (Na + K) in the bottom ash samples during the experiments. The long-term experiments are plotted directly after the corresponding 12 h experiment, and it should be recalled that the long-term experiment starts by simply shutting the forced bed regeneration off. The slope of the curve corresponds to the rate of alkali accumulation. In most cases, the rate is lower during the first 12 h. The fraction of alkali actually decreases in the reference ($ref_1$) and the low-dosage kaolin (kao2) cases. In all long-term experiments, alkali is accumulated. During the long-term tests, the accumulation rate is highest in the reference, sulphur and blast-furnace slag cases (refL CL, S6 CL, bfsL B, bfsL CL), while it is somewhat lower in the kaolin cases (kao2L CL, kao5L CL). The olivine cases differ between the bottom bed sample (oli B) and the cyclone-leg sample (oli CL), of which the former has a considerably higher accumulation rate.

### 3.3. Agglomeration temperatures

Fig. 8 shows the agglomeration temperatures of samples from the bed and the cyclone leg versus time. In the reference and olivine cases, the agglomeration temperature decreases, while in the kaolin

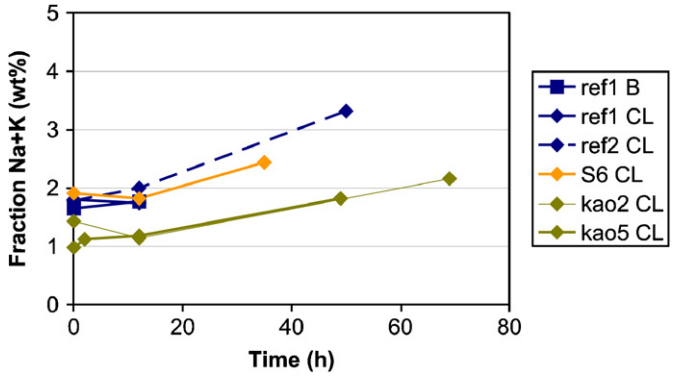


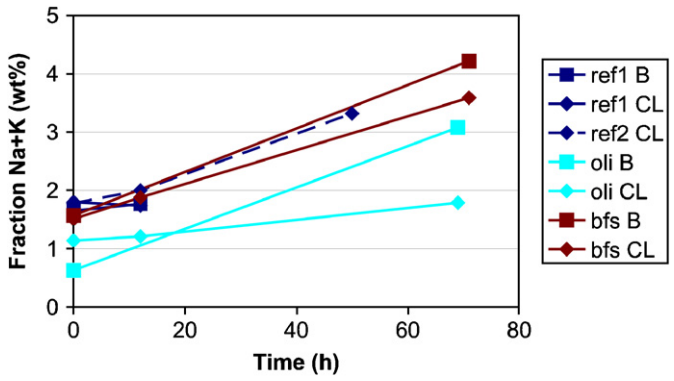


**Fig. 7.** Accumulation of alkali (Na + K) in the bottom ash.

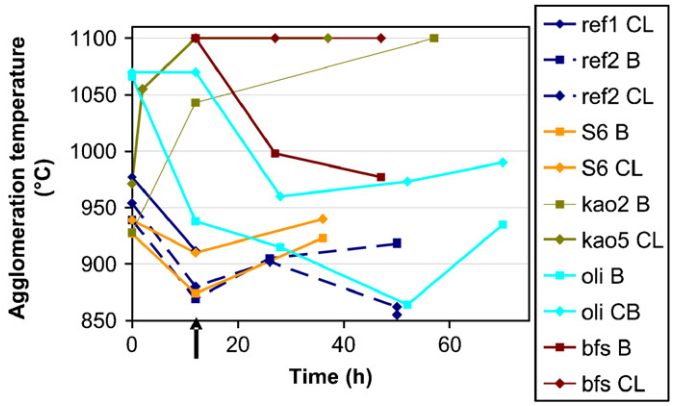


**Fig. 8.** Agglomeration temperatures of bed and cyclone-leg ash samples versus time. The arrow indicates when the forced bed regeneration was shut off.

cases, it increases. In the blast-furnace slag case, the agglomeration temperature is above the maximal experimental temperature during the first 12 h. Thereafter, the agglomeration temperature of the samples from the bottom bed decreases. In some of the tests, only one agglomeration temperature was achieved. The high ammonium sulphate sample (am5 CL12h) had an agglomeration temperature of 919 °C.

### 3.4. Bed particle structure

Cross-sections of particles in samples from the bottom bed and the cyclone, collected during the long-term tests, were analysed by SEM-EDX.

Figs. 9–11 show particles from bed samples and cyclone leg in the reference case. In Fig. 9 three of the particles contain high

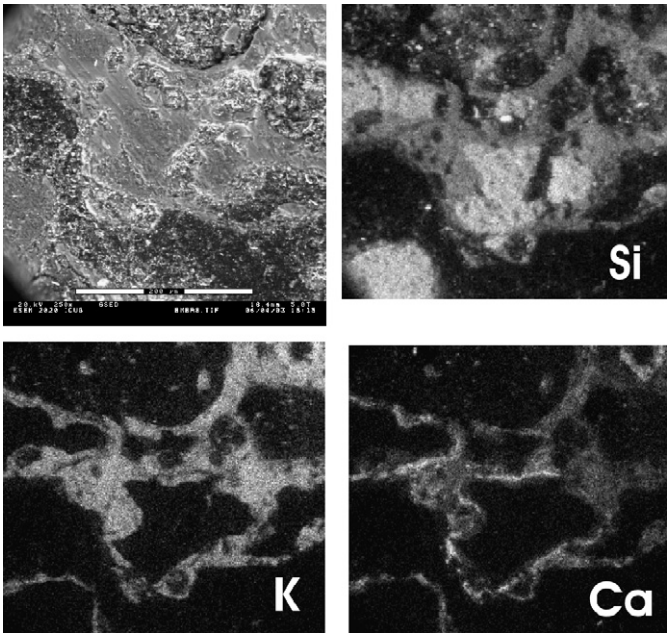


**Fig. 9.** Cross-sections of particles from the bottom bed in the refL case. The upper left is a SEM photograph and the others are element maps. The sides of the pictures correspond to 400 μm.

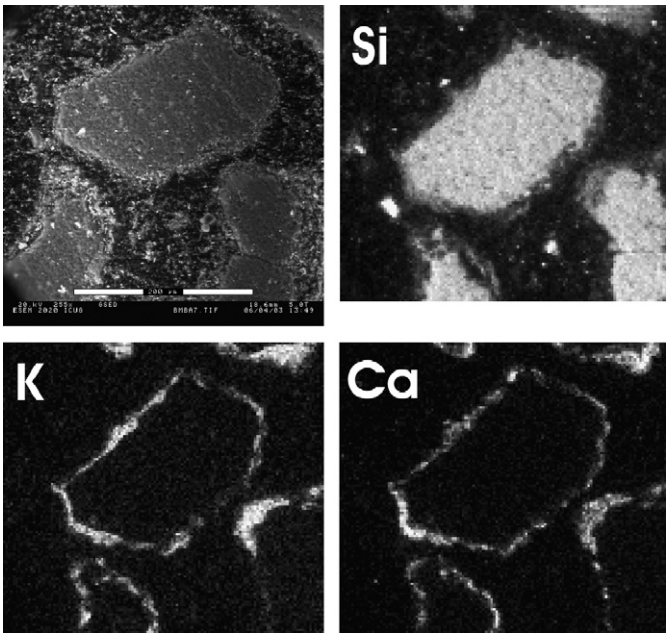


**Fig. 10.** Cross-sections of quartz particles from the bottom bed in the refL case. The upper left is a SEM photograph and the others are element maps. The sides of the pictures correspond to 400 μm.

amounts of silicon and oxygen (not shown). These are particles of the quartz-based bed material. Some particles are embedded in the molten ash, which mainly contains potassium, calcium and silicon. This molten ash probably comes from the straw, which is likely to have a low ash melting point because of its content of alkali and chlorine.

Fig. 10 shows cross-sections of quartz particles from the bottom bed in the reference case (refL). A layer containing potassium, calcium and silicon has formed on the particles. Calcium tends to be more concentrated in the outer part of the layer. Figs. 9 and 10 point at two possible mechanisms of agglomeration of bed particles: an ash melt that binds particles together and the formation of a sticky potassium-rich layer.

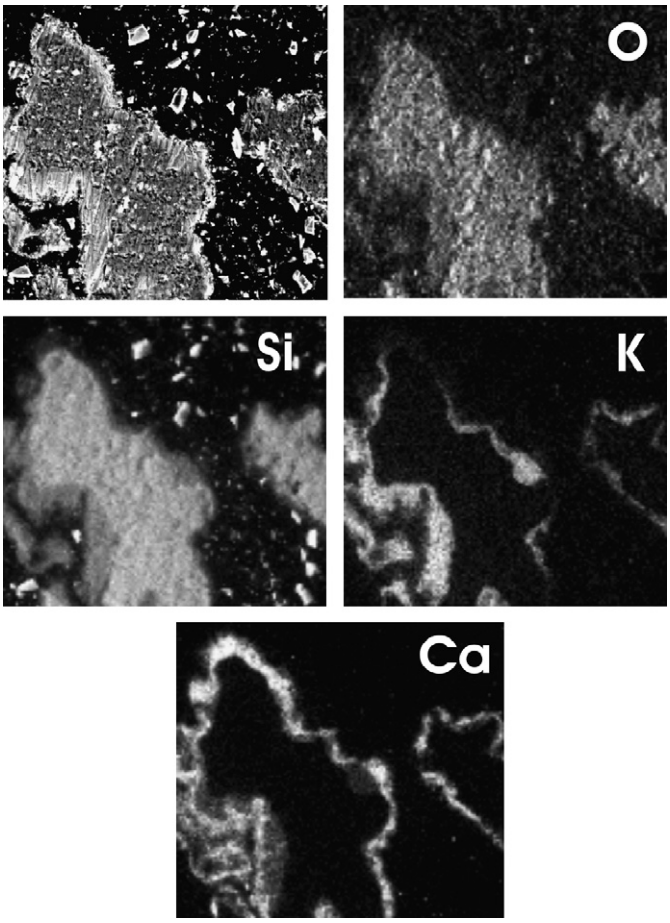


**Fig. 11.** Cross-sections of particles from the cyclone leg in the refL case. The upper left is a SEM photograph and the others are element maps. The sides of the pictures correspond to 400 μm.

Fig. 11 shows cross-sections of quartz particles from the cyclone leg in the reference case (refL). A layer has formed on the surface of the particles. The inner part of the layer contains mainly potassium and silicon, while the outer part contains mainly calcium. This points at the same agglomeration mechanism as Fig. 10, and ash melts were much less frequent in the cyclone-leg samples.

Cross-sections of particles from the bottom bed and the cyclone leg in the sulphur addition cases (S2L and S6L) show that a layer containing potassium, calcium and silicon has formed on the particles; very much like in the reference case.

Fig. 12 shows that particles in samples from the bottom bed during kaolin dosage (kao2L and kao5L) have a layer containing potassium and calcium on the surface of the particles. The inner part of the layer contains mainly potassium, and in some spots, aluminium. The outer part contains calcium. Silicon is present throughout the layer.

Fig. 13 shows particles from the bottom bed with olivine as bed material (oliL). Olivine particles are those that contain magnesium and iron. A layer containing calcium has formed on all particles, whereas potassium is not found on the olivine particles. Potassium and silicon have embedded two non-olivine particles, and calcium is concentrated in the outer part of this layer.

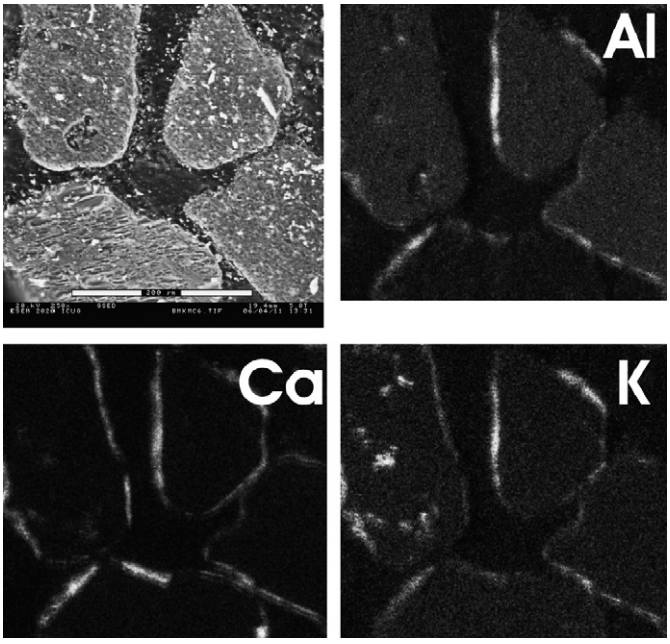


**Fig. 12.** Cross-sections of particles from the cyclone leg in the kao5L case. The upper left is a SEM photograph and the others are element maps. The sides of the pictures correspond to 400 μm.

Samples from the cyclone leg with olivine as bed material (oliL) show that potassium is found together with silicon in thick layers on non-olivine particles. A layer consisting of calcium has formed on most particles. Calcium is more concentrated in the outer part than in the inner part of the layer.

Fig. 14 shows cross-sections of particles from the bottom bed with blast-furnace slag as bed material (bfsL). Most particles have no layer at all, but on some particles, layers containing potassium, calcium and silicon have formed.

The results shown in Figs. 9–14 are collected in Table 4. Some observations:

- In all tests many particles are surrounded by a layer of a different chemical composition and physical structure that differs from the particle itself.
- K is present in the inner part of all layers.
- Ca is present in all layers, and more often in the outer part.
- Al is present in the layers when kaolin is added

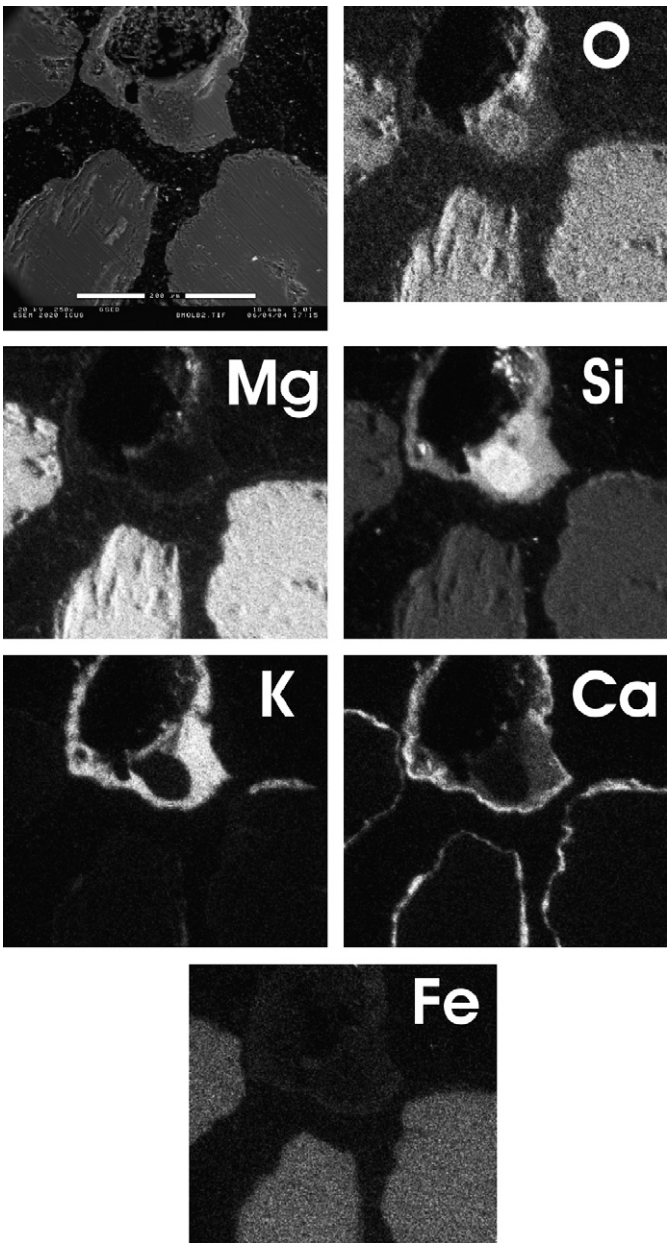


**Fig. 13.** Cross-sections of particles from the bottom bed in the oliL case. The upper left is a SEM photograph and the others are element maps. The sides of the pictures correspond to 400 μm.

### 3.5. Flue-gas composition

Figs. 15 and 16 show the concentrations of $SO_2$, HCl and alkali chlorides in the flue gas before the convection pass, and the concentrations of $SO_2$ and HCl in the stack. The gas temperature is around 800 °C upstream of the convection pass and about 150 °C in the stack. The long-term tests do not differ significantly from the corresponding 12 h tests.

In the reference cases, the concentrations of alkali chlorides and HCl are around 30 and 60 ppm, respectively. The fuels do not contain much sulphur and hence the concentration of $SO_2$ is only about 10 ppm. An increasing supply of ammonium sulphate to the flue gas has two effects apart from the obvious increase of the concentration of $SO_2$. The alkali chloride decreases: at the highest supply of ammonium sulphate it is below the measurable level (1 ppm). The concentration of HCl also decreases, which is probably an effect of the presence of ammonia, leading to formation of ammonium chloride. Otherwise formation of HCl would be the case while KCl is converted to $K_2SO_4$. Elemental sulphur lowers the concentration of alkali chlorides in the flue gas, but it does not affect HCl. Addition of kaolin has a small effect at the lowest dosage, but higher supplies of kaolin lead to lower concentration of alkali chloride. Using olivine sand instead of quartz-based sand causes higher concentration of alkali chlorides, while blast-furnace slag implies a slight decrease.

The emission of $SO_2$ is 10–30 ppm in most cases. When adding ammonium sulphate or elemental sulphur, the emission of $SO_2$ increases. The emission of HCl increases with increasing addition of kaolin or elemental sulphur, while ammonium sulphate has a decreasing effect. HCl decreases in most cases as the flue gas moves from upstream the convection pass to the stack. This is especially pronounced in the cases where the concentration of alkali chlorides is high.

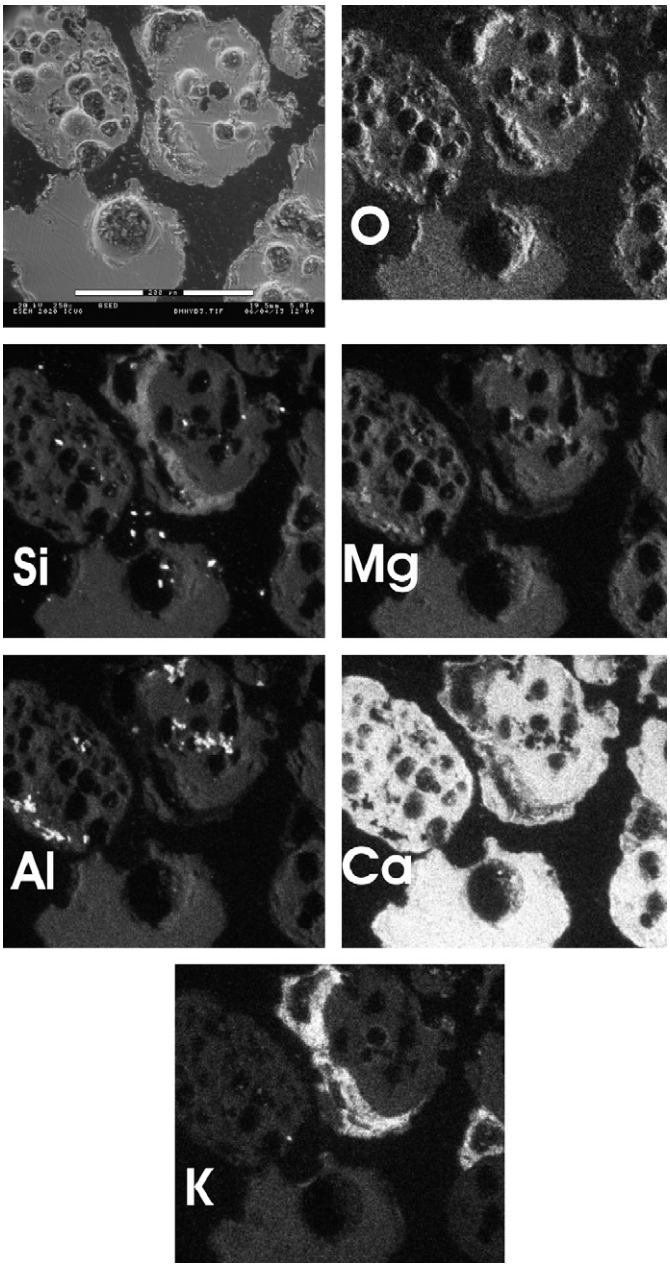


**Fig. 14.** Cross-sections of particles from the bottom bed in the bfsL case. The upper left is a SEM photograph and the others are element maps. The sides of the pictures correspond to 400 μm.

**Table 4**
Results of the analysis of cross-sections of particles from the bed material (bb, bottom bed; cl, cyclone leg)

| Experiment | Inner layer | Outer layer | Throughout layer | Spots |
|---|---|---|---|---|
| refL | cl: K, Si | cl: Ca | bb: K, Ca, Si | |
| kao2L | bb: K, Al, (Mg) | | bb: Ca<br>cl: Ca, K, Si, Al | cl: Mg |
| kao5L | bb: K | bb: Ca | bb: Si<br>cl: K, Al, Ca | bb: Al |
| oliL | bb: Ca<br>cl: Ca | | | K, Si |
| bfsL | | bb: Ca | | cl: K, Si Ca |
| S2L | bb: K, Ca, (Mn)<br>cl: K, Ca | | bb: Si<br>cl: Si | |
| S6L | cl: K, Ca | | cl: Si | |

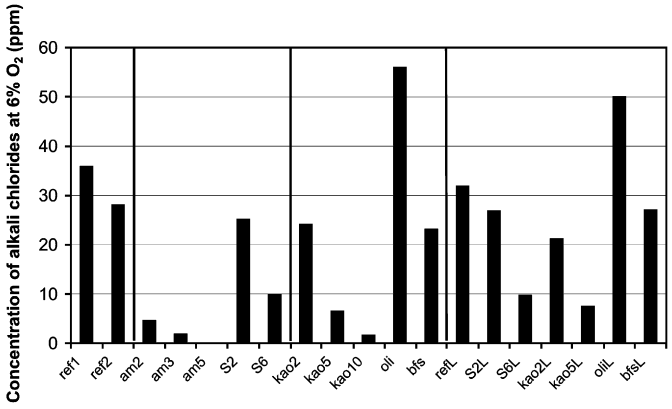


**Fig. 15.** Concentrations of alkali chlorides in the flue gas upstream of the convection pass.

### 3.6. Particles

#### 3.6.1. Size distribution

Fig. 17 shows mass size distributions of particles collected in the convection pass at about 250 °C (#13 in Fig. 1). Most cases exhibit a two-mode distribution between sub-micron and super-micron particles. The sub-micron particles are usually assumed to be formed by condensation of gaseous compounds as the flue gas is cooled, while the super-micron particles originate from substances that do not evaporate at the temperature in the furnace. Such substances may be present in the fuel ash and in additives. These particles may gain size and weight by condensation of the gases that form sub-micron particles.

There are more and larger sub-micron particles in the sulphur (S6), ammonium sulphate (am5) and olivine (oli) cases than in the reference ($ref_1$). The particle distribution in the blast-furnace slag (bfs) case is similar to the reference, and in the case of low addition of kaolin (kao2), the particles have the same size but the mass is lower. As more kaolin is added (kao5), the mass of the sub-micron particles decreases considerably, and at the highest addition of kaolin (kao10), no local maximum of the mass in the sub-micron range is found.

Super-micron particles are found in about the same amount in the reference, high addition of sulphur (S6) and ammonium sulphate (am5) cases. The more kaolin is added, the higher is the load of this type of particles. The change of bed sand to olivine or blast-furnace slag also gives rise to a higher load of particles larger than 1 μm than in the reference case.

#### 3.6.2. Composition

Fig. 18 shows the composition of particles collected in different cases. In all cases, sub-micron particles contain potassium together with chlorine and/or sulphur. In super-micron particles, the fractions of potassium, chlorine and sulphur decrease, while calcium, silicon and other elements, specific for the case in question, dominate.

Potassium and chloride dominate in sub-micron particles in the reference case (Fig. 18a), the kaolin cases (Fig. 18d and e), the olivine case (Fig. 18f) and the blast-furnace slag case (Fig. 18g). Addition of sulphur in the form of elemental sulphur (Fig. 18c) lowers the chlorine content and the addition of ammonium sulphate (Fig. 18b) eliminates chlorine. It is difficult to explain why the smallest particles should contain iron and aluminium, so this should be regarded as an artefact. A comparison of kao2 (Fig. 18d) and kao5 (Fig. 18e) shows that a higher addition of kaolin lowers the fraction of potassium and chlorine in all but the smallest particles. In the oli case, the potassium and chlorine dominate in particles up to 1.14 μm, while in the ref and bfs cases, the corresponding diameter is 0.45 μm.

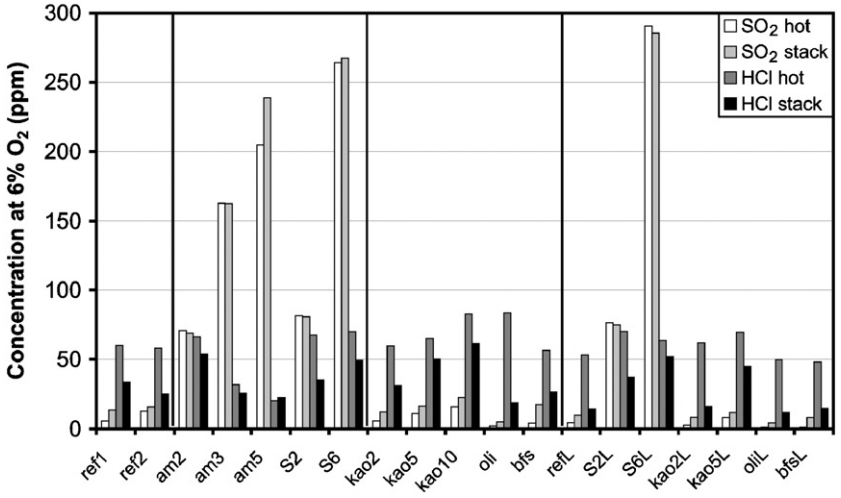


**Fig. 16.** Concentrations of $SO_2$ and HCl in the flue gas upstream of the convection pass (hot, #12 in Fig. 1) and in the stack (#14 in Fig. 1).

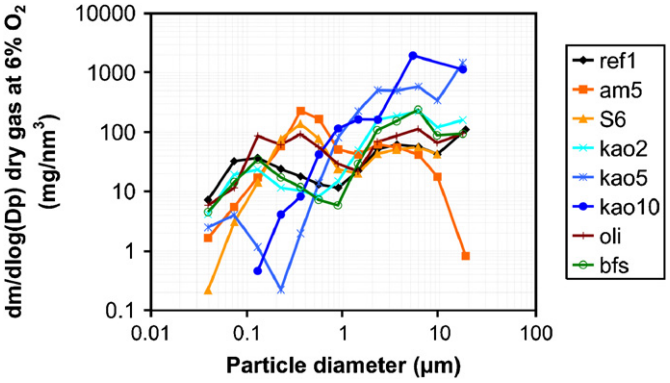


**Fig. 17.** Mass size distributions of particles collected at about 250 °C in the convection pass.

In the ref, am5 and S6 cases, the super-micron particles contain increasing fractions of calcium and silicon. In the kao2 and kao5 cases, these particles contain increasing fractions of aluminium, which is evidence of kaolin. In the oli and bfs cases, the content of the super-micron particles reflect the composition of the bed material. Hence, in the oli case, the particles contain magnesium, iron and silicon, and in the bfs case, they contain calcium, aluminium and magnesium.

### 3.7. Deposits

#### 3.7.1. Mass gain

Fig. 19 shows the mass gain on average of deposit rings. The deposit growth is lowest in the reference cases irrespective of exposure time. The growth is slightly higher in the blast-furnace slag and medium kaolin cases (bfs and kao5). Significantly higher growth is observed in the low kaolin, sulphur and olivine cases (kao2, S and oli). The long-term olivine case (oliL) gives rise to the highest deposit growth. There is no clear trend as for the importance of exposure time for deposit growth. In the reference cases, there is a slight decrease of the growth as the exposure time increases from 4 to 12 h. In the olivine cases there is a significant increase of the growth when the exposure time increases from 12 to 22 h. In the blast-furnace slag cases there is a significant decrease of the deposit growth when the exposure time increases from 4 to 12 h, but thereafter it tends to increase. In the sulphur cases there is no clear trend.

#### 3.7.2. Composition

In Fig. 20 the deposits are given as elements. Potassium and chlorine dominate unless sulphur or enough kaolin is added. When ammonium sulphate or elemental sulphur is added, sulphur is found instead of chlorine in the deposits. In the low kaolin case (kao2) there is almost as much chlorine as in the reference case. Adding more kaolin (kao5) eliminates chlorine in the deposits.

Fig. 21 shows SEM-EDX maps over the deposit surface on the steel rings in different cases. The time of exposure differs, but the major purpose of these measurements is to establish the correlation between elements and thereby the compounds present. In the ref case (Fig. 21a) there is a strong correlation between potassium and chlorine. The same result was attained in the refL case. After 12 h of exposure, the low dosage of sulphur (S2) showed a stronger correlation between potassium and chlorine than with sulphur. After 21 h the correlation has shifted towards sulphur (b). A higher dosage of sulphur (S6) gives rise to a strong correlation between potassium and sulphur after 4 h (c). Addition of ammonium sulphate also implies a strong correlation between potassium and sulphur, even though it is the lowest dosage tested and only 4 h (d). In the kao2 case, the deposits contain aluminium, which is evidence of kaolin (e). However, at this low dosage, potassium is more correlated with chlorine than with aluminium. In the olivine and blast-furnace slag cases (f and g), potassium clearly correlate with chlorine, but also to some extent with sulphur.

To summarize, the elemental and SEM-EDX analyses show that most of the deposits consist of KCl. If sulphur is added in the form of ammonium sulphate or elemental sulphur, potassium is found in connection with sulphur, which is likely to be $K_2SO_4$.

## 4. Discussion

### 4.1. Bed agglomeration

#### 4.1.1. The reference cases

In the reference cases, the potassium that is accumulated in the bed material has reacted with silica in the bed sand, forming potassium silicates. This is concluded from the correlation of potassium and silicon in the SEM-EDX analyses of the bed particles (Figs. 10 and 11). After some time of operation this gives rise to a sticky

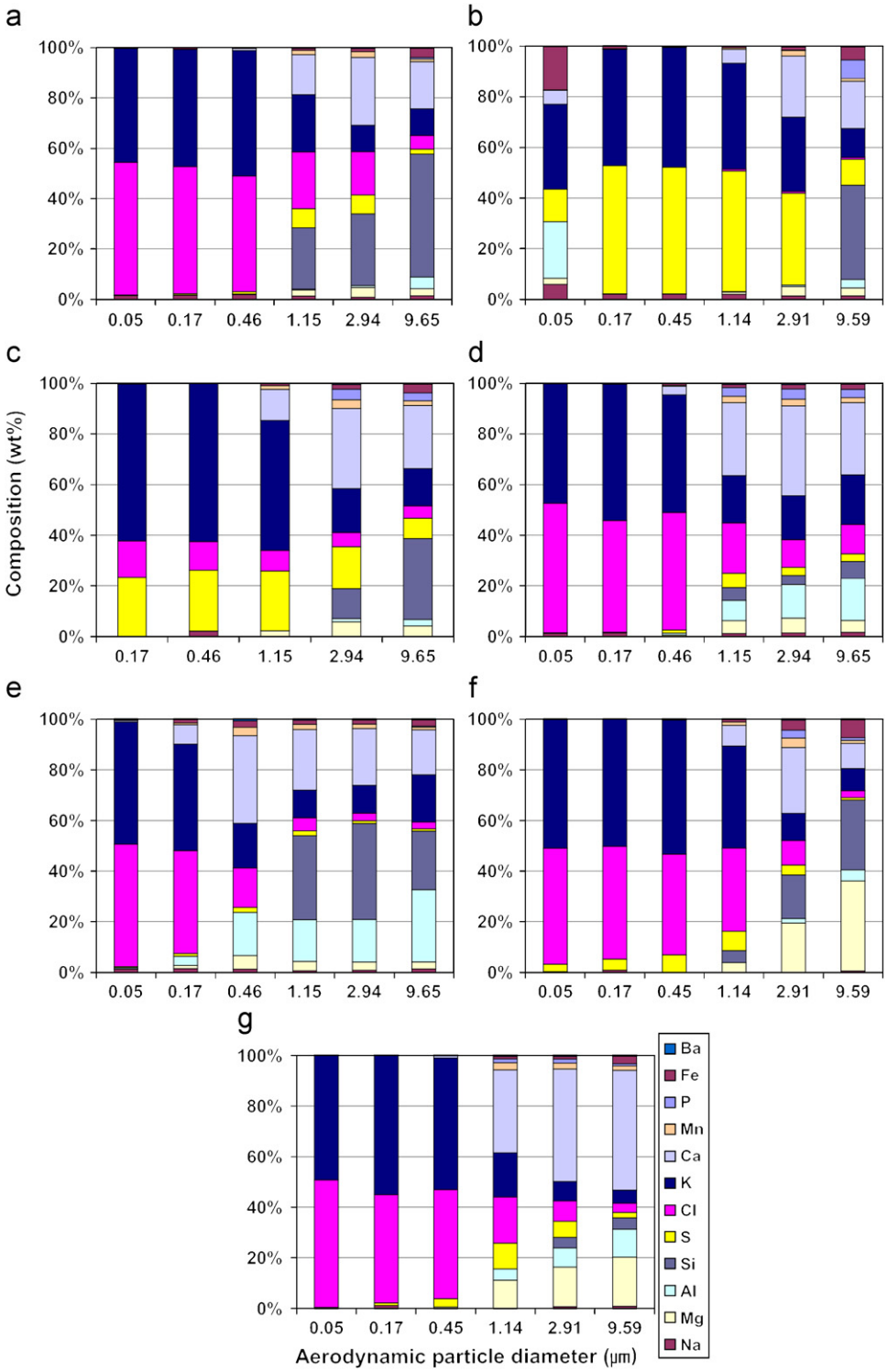


**Fig. 18.** Composition of particles of different sizes in the cases (a) $ref_1$, (b) am5, (c) S6, (d) kao2, (e) kao5, (f) oli and (g) bfs. In each bar, elements are situated in the same order as in the legend to the right of diagram (g).

surface on the bed particles which lowers the agglomeration temperatures (Miles et al., 1996; Öhman et al., 2000). Calcium, which constitutes a substantial part of the fuel ash, adheres to the bed particles because of the sticky surface layer. Calcium should counteract the stickiness of the particle, and hence, lower the agglomeration risk (Öhman et al., 2000). The accumulation of alkali in the bed is small in the reference cases and well below the theoretical maximum of 2.7 wt%, which would be if all alkali supplied with the fuel were accumulated in the bed material. Some of the alkali leaves the furnace in the form of gaseous chlorides, as shown in Fig. 15. Despite this, the decrease of the agglomeration temperature is significant. In the long-term test (refL) the accumulation exceeds 2.7 wt% because the bed regeneration was shut off, but the effect on the agglomeration temperature is unclear. This shows that even though alkali is important, it is not the only parameter that affects agglomeration. After the formation of the inner surface layer of alkali silicates

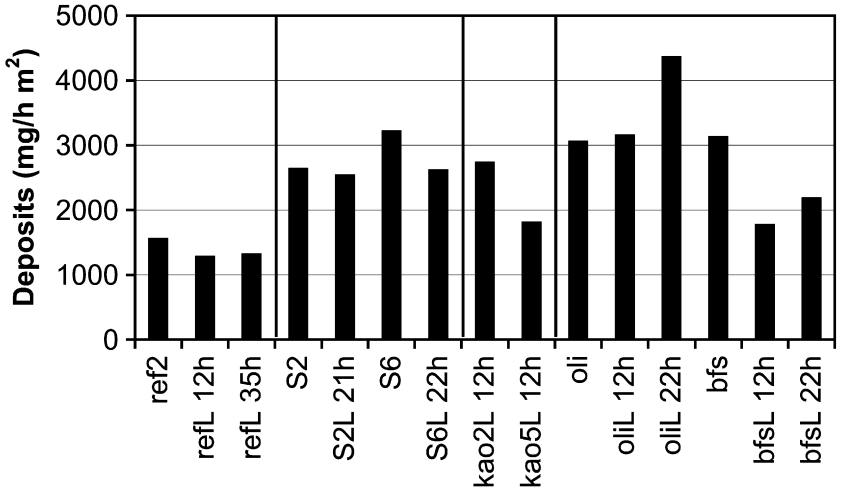


**Fig. 19.** Mass gain on deposit rings per unit time and surface area. Time of exposure is 4 h unless otherwise noted.

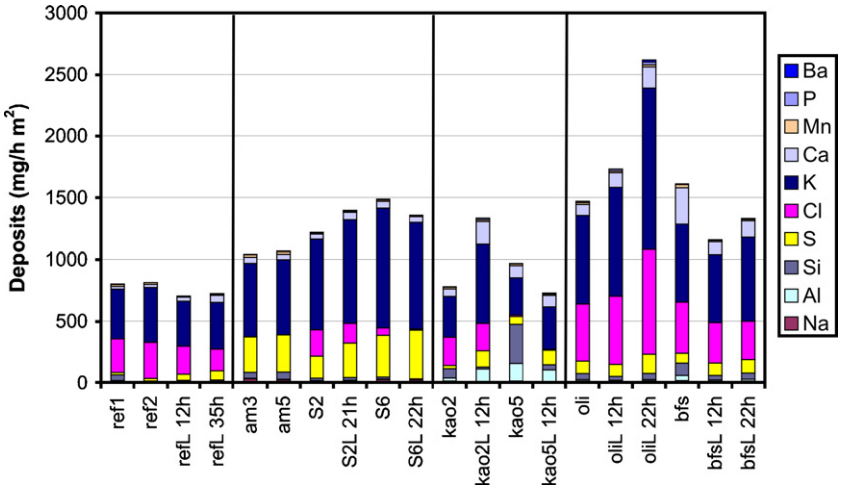


**Fig. 20.** Deposits given as elements. Of major elements, oxygen and carbon are not included.

and the outer surface layer of calcium, additional alkali may have a smaller effect on the agglomeration temperature. Straw pellets provide an additional agglomeration mechanism because of the formation of melted ash lumps. The bed-ash samples contain straw pellets in different degrees of conversion. The ash of the straw pellet melts during char combustion and captures bed particles in its vicinity. This could cause formation of larger lumps, but such lumps were not observed. Instead, the ash melts are small (Fig. 9) and even smaller lumps were found in the ash samples from the cyclone leg (Fig. 11). Experience from the present boiler shows that the conditions during the reference cases (20% straw on energy basis) lead to agglomeration in the particle seal, causing a shut-down within a week of operation. Therefore, to be able to fire straw pellets and other problematic fuels, the observed accumulation of alkali and the decreasing agglomeration temperatures must be counteracted by additives or by a better choice of bed material.

*4.1.2. The ammonium sulphate cases*

The effect of ammonium sulphate on bed agglomeration was not expected to be large, because the ammonium sulphate was supplied between the furnace and the cyclone and should form small particles carried by the flue gas. Hence, the ammonium sulphate would be in contact with the bed particles for only a short time. However, the agglomeration temperature of the cyclone-leg sample taken after 12 h was 919 °C, which is higher than in the reference cases. The fraction of alkali is lower in the bed and cyclone-leg samples during ammonium sulphate addition than in the reference samples, and therefore an effect of ammonium sulphate on bed agglomeration cannot be ruled out. The mechanism behind this does not require that sulphur stay in the bed, since no sulphur was found in the bottom ash and little in the cyclone-leg sample. The ammonium sulphate reacts with gaseous alkali compounds, such as KCl, as shown in Fig. 15. From an equilibrium point of view, the lower concentration of KCl in the flue gas should favour the release of alkali from bed particles and unburnt fuel particles. This suggests that ammonium sulphate increase the agglomeration temperature. However, the effect is small, and the agglomeration temperature probably decreases during the test. On the other hand, the effect might become larger if the ammonium sulphate were added in the upper middle part of the furnace. This needs to be examined further.

*4.1.3. The sulphur cases*

The effect on the composition of bottom ash from addition of elemental sulphur is small even at the highest addition rate (6S). The agglomeration temperature decreases during the first 12 h, and exhibits much the same behaviour as in the reference samples. In

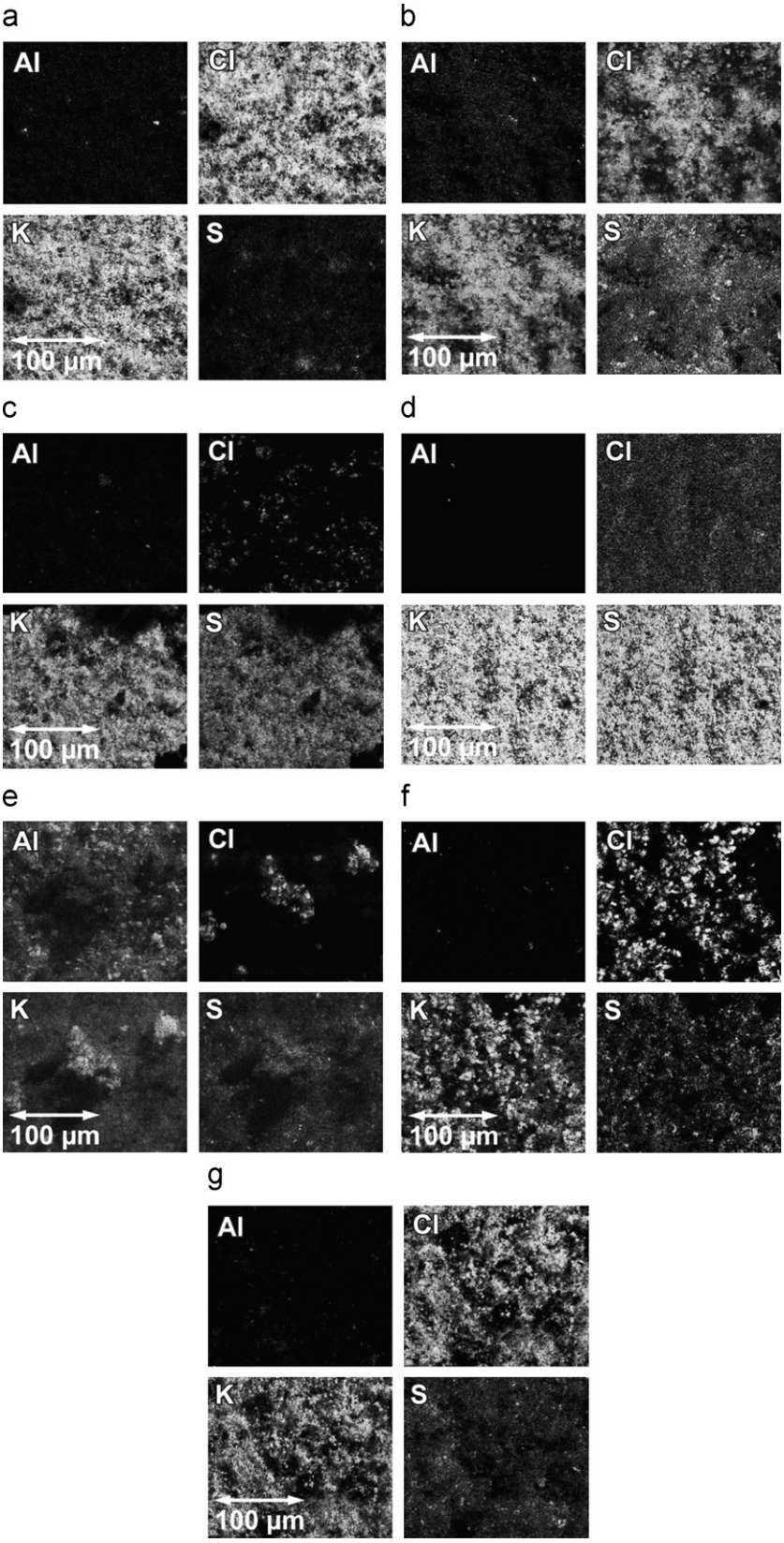


**Fig. 21.** SEM-EDX maps of deposits collected during exposure to the flue gas in the cases (a) reference (ref) 4 h, (b) low sulphur (S2L) 21 h, (c) high sulphur (S6) 4 h, (d) low ammonium sulphate (am2) 4 h, (e) low kaolin (kao2) 12 h, (f) olivine (oliL) 21 h, (g) blast furnce slag (bfs) 21 h.

the long-term test (6SL), the alkali fraction of the cyclone-leg samples increases. During this period, the agglomeration temperature increases, which compares with the $ref_2$ B sample. The bed particles also have approximately the same structure as in the reference

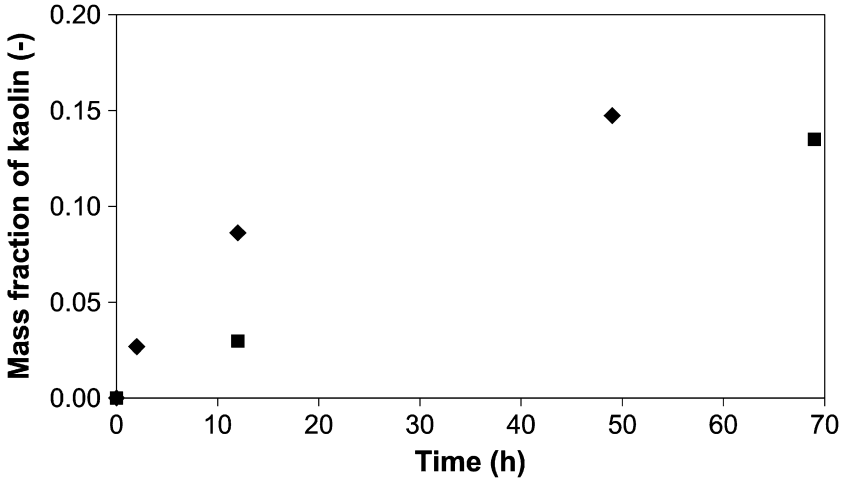


**Fig. 22.** Content of kaolin in cyclon-leg samples during the kao2 case (squares) and the kao5 case (rhombi).

case. The mechanism behind these effects is not clear, but sulphur could react with potassium and thereby remove it from the bed as e.g. sulphate. However, the resemblance to the reference case shows that sulphur has a small importance for agglomeration.

*4.1.4. The kaolin addition cases*

In the low-kaolin case (kao2), the mass fraction of alkali decreases in the ash samples from the cyclone leg, whereas in the medium-kaolin case (kao5), it increases. This apparently contradictory behaviour can be explained by the different mass fractions of accumulated alkali at the start of the test. At the end of the tests, the mass fractions were almost the same and below 3.1 wt%, which is the theoretical maximum. The presence of aluminium in the surface layers of the bed particles shows that kaolin interacts with the material. Again, it is likely that alkali forms a sticky layer by reaction with silicon. Then kaolin adheres to the surface and reacts with the potassium, whereby potassium aluminium silicates are formed (Davidsson et al., 2007a; Steenari and Lindqvist, 1998). These compounds have higher melting points than potassium silicates, and this results in an increase of the agglomeration temperatures in the kao2 case, and especially in the kao5 case. Gaseous potassium compounds may also react directly with kaolin particles, which thereafter adhere to the surface of the bed particles (Öhman and Nordin, 2000). The concentration of gaseous alkali chlorides in the flue gas, shown in Fig. 15, decreases as the dosage of kaolin increases. The kaolin applied is a fine powder, and it is expected to partly be carried away by the flue gas. The reaction lowering the concentration of alkali chlorides may therefore take place in the upper part of the furnace or between the furnace and the measurement spot for gaseous alkali chlorides (#12 Fig. 1). In the long-term tests (kao2L and kao5L), alkali is accumulated in the bed material at approximately the same rate. This supports the notion that kaolin particles are entrained by the flue gas while they capture alkali. Instead of reacting with potassium, the chlorine forms HCl, the concentration of which increases with increasing supply of kaolin (Fig. 16).

The experimentally determined aluminium content in the cyclone-leg samples (Fig. 3) recalculated to kaolin reaches a mass fraction in the bed of about 0.15 at the end of the experiments, as shown in Fig. 22. Agglomeration temperatures $\geqslant$1100 °C should be unproblematic during full-scale operation. Such temperatures were attained in the agglomeration furnace (cf Section 2.5) after 12 (kao5) and 57 (kao2L) h, or even earlier in the kao2L case since the temperature was not examined between 12 and 57 h. Analysing Fig. 22, it can be concluded that a mass fraction of kaolin of about 0.1 is sufficient to keep the agglomeration temperature $\geqslant$1100 °C. This occurs after less than 12 h in the kao10 case and around 40 h in the kao2 case. The lowest addition of kaolin that can meet this requirement at a bed removal rate of 70 kg/h is about 7 kg/h, which corresponds to a molar input of kaolin to alkali of about 0.85 times the stoichiometric ratio.

The kao2 and kao5 cases have a similar effect on the bed material, even though the agglomeration temperature rises faster in the kao5 case because of faster increase of the kaolin fraction in the bed. This shows that there is an upper limit above which additional kaolin has little effect on bed agglomeration.

*4.1.5. The olivine cases*

Exchanging the bed of quartz-based silica sand for olivine sand provides a chemically different environment for the fuel and the compounds released during combustion. For example, the agglomeration temperature is about 1070 °C initially, which is at least 100 °C higher than for the silica sand in the reference cases (Fig. 8). Still, alkali is captured in the bed material (Figs. 5 and 7), but it does not react with the olivine particles. Rather, it is found in thick layers on and between the other bed particles (Fig. 13). The capture of alkali is considerably higher in the bed ash than in the cyclone-leg ash (Fig. 5), which makes it likely that the layers are caused by melted straw pellet ash, which is present in a higher amount in the bed. This makes the agglomeration temperature of the bed ash drop about 130 °C during the 12 h test, while the cyclone-leg ash is unaffected (Fig. 8). However, in the long-term test (oliL) the cyclone-leg ash also reaches a lower agglomeration temperature even though it is always considerably higher than that of the bed ash throughout the whole test period. These findings are consistent with observations during firing of wood fuels in pilot-scale tests in a CFB (Almark and Hiltunen, 2005). Alkali that is not present in the ash melt does not react with the olivine. Instead, it forms gaseous alkali chlorides to a larger extent than in the reference cases, as shown in Fig. 15.

*4.1.6. The blast-furnace slag cases*

Blast-furnace slag, like olivine sand, provides a chemically different environment for the compounds released from the fuel. The agglomeration temperature after 12 h of the experiments is >1100 °C in the bed ash and the cyclone-leg ash. It is concluded that the corresponding temperature at 0 h was >1100 °C as well. The behaviour of ash and alkali is similar to that in the case of olivine sand. The alkali that is accumulated in the bed material, does not react with the surface of the bed particles (Fig. 14); an observation which is in

accord with findings in bench-scale experiments (Brus et al., 2004). Instead, it is found in ash melts. This affects the agglomeration temperature of the bed ash, but the cyclone-leg ash still has an agglomeration temperature >1100 °C after 47 h of operation without bed regeneration (bfsL) (Fig. 8). The performance of blast-furnace slag is considerably better than quartz-based sand, also in accord with bench-scale experiments (Brus et al., 2004). The concentration of gaseous alkali chlorides is not, as opposed to the case with olivine sand, higher than in the reference case. This can be explained by the slightly higher alkali accumulation in the bed material.

### 4.2. Deposits

#### 4.2.1. The reference cases

The amount of deposit is relatively small in the reference case (Fig. 19) but the deposit consists almost entirely of KCl. This is concluded from the SEM-EDX analysis (Fig. 21a), which shows a clear correlation between potassium and chlorine. A deposit of KCl is undesired because of its liability to favour corrosion. Deposition and corrosion during firing of straw are well known (Hansen et al., 2000; Michelsen et al., 1998). This means that the present fuels should not be fired without countermeasures, preventing deposits dominated by KCl. It is difficult to establish a certain concentration of gaseous alkali chlorides below which the deposit/corrosion could be controlled. Such a study would have to include long-term corrosion tests and is outside the scope of the present work. Instead, a countermeasure is regarded successful if the concentration of alkali chlorides in the flue gas is below 5 ppm, which is approximately the flue-gas concentration upon firing only wood chips or wood pellets. Based on experience in the present boiler these are unproblematic fuels with respect to alkali.

#### 4.2.2. The ammonium sulphate cases

The lowest dosage of ammonium sulphate (am2) is enough to keep the concentration of alkali chlorides at 5 ppm (Fig. 15). A higher dosage makes the concentration even lower but also rises the emission of $SO_2$. The mass distribution of sub-micron particles is shifted to larger diameters compared with the reference case (Fig. 17). This can be explained with the fact that the amount of substance, liable to condense, is much larger because of the additive. It also explains the higher deposition rate compared to the reference case. The sub-micron particles in the flue gas contain potassium and sulphur, but no chlorine (Fig. 18b). The deposits (Fig. 20) and the SEM-EDX analysis (Fig. 21d), which shows a strong correlation between potassium and sulphur, also point at the formation of $K_2SO_4$. From a corrosion point of view, deposits of $K_2SO_4$ are less hostile than those of KCl. The present findings are in accord with observations made during firing of bark and waste in a full-scale CFB boiler (Broström et al., 2007). Both KCl and HCl decrease as the dosage of ammonium sulphate is increased. This suggests formation of gaseous $NH_4Cl$.

Chlorine is liable to react with alkali to form chlorides, but sulphur competes with chlorine for alkali and forms sulphates. The resulting amounts of chlorides and sulphates depend upon the inflow of sulphur and chlorine at a given inflow of alkali. Therefore, as long as available alkali is in excess of chlorine and sulphur, the inflow ratio S/Cl is more important than the actual inflow of alkali. This is important for the calculation of the cost of the dosage. In the am2 case, the S/Cl ratio was 2.1, which can be taken as a minimum to reduce KCl below 5 ppm in the flue gas. This is about $\frac{1}{3}$ of the same ratio in the 6S case, in which the concentration of KCl was 10 ppm. It is concluded that the formation of $SO_3$ from $SO_4^{2-}$ is considerably more effective than that from $SO_2$. If less alkali is available, then less sulphur is needed, or if a high amount of calcium is present, then more sulphur is needed, because of sulfation of calcium. To summarize, it is important for the operation of the plant to control the inflows of alkali, chlorine, sulphur and calcium. The cost of counteracting possible alkali-related problems depends on all these inflows.

#### 4.2.3. The sulphur cases

The effect of sulphur on the concentration of KCl is significant but smaller than that of ammonium sulphate. None of the tested dosages of sulphur could meet the requirement that the concentration of KCl should be $\leqslant 5$ ppm. During the highest dosage (S6), the concentration of KCl reached 10 ppm, while the emission of $SO_2$ was in the same range as during dosage of ammonium sulphate.

As in the case of ammonium sulphate, the amount of substance that can form particles (Fig. 17) and the deposition rate (Figs. 19 and 20) are larger than in the reference cases. Therefore the mass distribution is shifted from sub-micron particles to larger particles and higher particle load. $SO_2$ and chlorine react with alkali and form sub-micron particles, which consist almost entirely of potassium, chlorine and sulphur (Fig. 18c). The proportion between these elements is approximately maintained also in the super-micron particles, but these also contain other ash elements. In the S2 and S2L cases, the deposits contain potassium, chlorine and sulphur (Fig. 20) and the SEM-EDX analyses show a correlation between potassium and chlorine as well as between potassium and sulphur (Fig. 21b). It is concluded that the particles, as well as the deposits, contain KCl and $K_2SO_4$. In the S6 case very little chlorine is found in the deposits (Fig. 20) and in the corresponding long-term test (S6L), there was no chlorine. The SEM-EDX analysis in the 6S case (Fig. 21c) shows a strong correlation between potassium and sulphur, while the chlorine signal is weak. It shows that the deposit mainly consists of $K_2SO_4$, and little, if any, KCl. This is interesting because the KCl in the flue gas is expected to lead to deposition of KCl.

#### 4.2.4. The kaolin cases

As the dosage of kaolin is increased, the increasing concentration of super-micron particles of kaolin (Fig. 17) lowers the concentration of gaseous KCl (Fig. 15). This can occur by two mechanisms:

(a) reaction between KCl (g) and kaolinite (which is the essential aluminium silicate in kaolin) forming potassium aluminium silicate and HCl (Steenari and Lindqvist, 1998);
(b) condensation of KCl (g) on kaolin particles, and possibly subsequent reactions as in mechanism (a) between KCl (l) and kaolinite (Valmari et al., 1999).

In the present case, the temperature where gaseous alkali chlorides are measured is too high for condensation to take place (mechanism (b)). The concentration of sub-micron particles decreases with dosage of kaolin (Fig. 17) despite the significant fraction of such particles in the kaolin itself. Removal of KCl (g) according to mechanism (a), as well as growth of super-micron particles by collision with sub-micron particles, may explain this. The composition of particles of different sizes shows that the low kaolin dosage (kao2) is unable to prevent the formation of sub-micron particles, consisting mainly of KCl (Fig. 18d), and deposits containing KCl (Fig. 21e). The super-micron particles contain less potassium and chlorine, but it is likely that a substantial fraction of these elements still occur as KCl. At a higher dosage (kao5), on the other hand, only particles below 0.5 μm contain a substantial amount of KCl, whereas super-micron particles contain considerably more potassium than chlorine (Fig. 18e). The increasing fraction of aluminium in larger particles shows that potassium aluminium silicates, for example $KAlSiO_4$ or $KAlSi_3O_8$, (Davidsson et al., 2007a; Steenari and Lindqvist, 1998), have been formed. The interpretation of this is that the addition of kaolin has to exceed a certain amount to meet the requirement that the concentration of alkali chlorides should be below 5 ppm in the flue gas. The concentrations of gaseous KCl in the kao5 and kao10 cases were 7 and 2 ppm, respectively. Assuming a linear relationship between

the concentration of alkali chlorides and the dosage of kaolin in the range 2–7 ppm, 5 ppm would require a dosage of kaolin, corresponding to a kaolin/alkali ratio of 7.2 times the stoichiometric ratio.

#### 4.2.5. The olivine cases

Olivine as bed material gives rise to higher concentrations of alkali chlorides in the flue gas than in the reference cases with silica sand (Fig. 15): olivine sand captures less alkali than silica sand, and, as a result, more alkali reaches the gaseous phase. As a consequence, there are more sub-micron particles in the olivine case (Fig. 17) with the main constituents potassium, chlorine and some sulphur (Fig. 18f). The high concentration of alkali chlorides in the flue gas and high load of sub-micron particles give rise to a higher rate of deposition (Fig. 19), also consisting mainly of potassium, chlorine and some sulphur. The SEM-EDX analysis (Fig. 21f) shows that potassium and chlorine correlate in the deposits. There is also a weak correlation between potassium and sulphur. Evidently, most potassium and chlorine is present as KCl in particles as well as in deposits, and that there is also some $K_2SO_4$. Though olivine reduces the agglomeration tendency of the bed, it has a negative effect on deposition. Use of olivine sand with the present fuels is likely to cause deposition/corrosion.

#### 4.2.6. The blast-furnace slag cases

Blast-furnace slag as bed material yields slightly lower concentration of alkali chlorides, $SO_2$ and HCl in the flue gases compared with the reference cases (Fig. 15). This is in agreement with the observation that binding of alkali in the bed is about the same for blast-furnace slag and silica sand (Fig. 7). The mass distribution of sub-micron particles is also similar to that in the reference cases, while the concentration of super-micron particles is higher (Fig. 17). The explanation is probably that the attrition of the bed material is as high as 13 kg/h (Table 3). The sub-micron particles consist of potassium and chlorine. The molar ratio of potassium to chlorine is about one for all particle sizes, but super-micron particles also contain ash elements (Fig. 18g). Furthermore, the presence of calcium, magnesium and aluminium shows that these particles partly emanate from the fine fraction and from attrition of the blast furnace slag. Due to the high load of super-micron particles, the deposition rate is considerably higher than in the reference cases (Figs. 19 and 20).

The deposits contain more chlorine and potassium, as well as ash elements and elements from the blast-furnace slag than in the reference case (Fig. 20). The higher rate of deposition is explained by the higher particle load, especially if the deposition starts with the formation of a sticky layer of KCl. The higher deposition rate of KCl is unexpected because there was slightly less gaseous KCl in the flue gas. However, the gaseous KCl can condense on larger particles and sub-micron particles may coalesce with larger particles, which thereafter are deposited. The SEM-EDX analysis shows a strong correlation between potassium and chlorine, and evidently KCl is the major substance in deposits and sub-micron particles. Also present are sulphur, calcium and magnesium.

The high load of deposition and its major constituent KCl show that blast-furnace slag is unsuitable as bed material to avoid deposition problems when firing alkali-rich fuels.

## 5. Required dosages and their costs

The aim of the additives and the alternative bed materials is to keep the agglomeration temperature above the temperature in the furnace. Even if bed temperature in the present case was 850 °C, other boilers may operate at higher temperatures. Furthermore, the temperature may locally exceed the average. This is especially the case in the vicinity of a burning fuel particle. The agglomeration temperatures of the bed samples achieved experimentally should not be interpreted as the exact temperature at which the bed would agglomerate in the boiler, but if a certain action leads to a higher agglomeration temperature then a lower risk of agglomeration is expected. Altogether, one cannot establish a certain agglomeration temperature that would safely avoid agglomeration. Nonetheless, analysing Fig. 8, it is obvious that only kaolin addition and blast-furnace slag meet the requirements.

Even the lower dosage of kaolin (kao2 and kao2L) makes the agglomeration temperature increase to > 1100 °C after 57 h of operation without forced bed regeneration. In the kao2 case the actual ratio of kaolin to alkali was 1.8 times the stoichiometric ratio (Table 3) but the analysis shows that a ratio of 0.85 should be sufficient. The price for the kaolin was 270$/ton. The deposition fee for ashes can vary depending on classification and domestic rules. It is assumed to be 100$/ton. With an inflow of potassium of 64 mol/h the kaolin demand would be about 7 kg/h. This corresponds to a cost of 2.6$/h in the present case. This is 0.040$/mol potassium and 0.43$/MW h.

The blast-furnace slag consists partly of a fine fraction, which is separated in the cyclone, ending up in the fly ash. Based on the fly ash flows in the bfs and bfsL cases it is concluded that the fine fraction constitutes 30–40% of the mass. This means that of the 149 kg/h of input of blast-furnace slag, about 90 kg/h stays in the bed. A commercial product should be better prepared, e.g. by sieving, and therefore the cost of this loss of bed material is not taken into account here. Instead a loss of 10 wt% due to attrition is assumed. The maximal rate of loss due to attrition is 13 kg/h (Table 3). The price of the blast furnace was 240$/ton. With the same deposition fee as in the kaolin cases, this corresponds to a cost of 4.42$/h, equaling 0.71$/MW h. The agglomeration temperature of the bed ash in the bfsL case decreases considerably when the bed regeneration is shut off (Fig. 8). To avoid this, a higher regeneration of blast-furnace slag is needed, but it is too expensive and probably unnecessary to use 90 kg/h as in the bfs case. Comparing with silica sand, the price of which presently is 65$/ton, the economic break-even point of input of blast-furnace slag would be about 25% of that of the silica sand. Judging from Fig. 8, the input of silica sand that is needed to keep the bed agglomeration temperature constant, is far higher than 90 kg/h. Therefore, even though it is not possible to tell exactly from the data available, blast-furnace slag can be economical compared with silica sand.

In the reference case, it was shown that the presence of KCl in flue gas and the in the deposits was unacceptable from a deposition/corrosion point of view. The alternative bed materials made the impact of KCl worse. The kaolin and the sulphur additives were shown to counteract the deposition of KCl. A molar input of kaolin to alkali of 7.2 times the stoichiometric ratio would be enough to fulfil the requirement of a flue-gas concentration of KCl $\leqslant$ 5 ppm. Based on a price on kaolin of 270$/ton and a deposition cost of 100$/ton, the cost for such a dosage would be 20$/h. This corresponds to 0.3$/mol potassium and 3.4$/MW h.

The mechanism of sulphur/sulphate is more complex than that of kaolin, which simply reacts with and binds potassium. Sulphur and sulphate compete with chlorine for potassium in the gas phase, and calcium, which is always present, readily reacts with sulphur. Therefore, the cost cannot be given per unit potassium. Addition of sulphur/sulphate increases the emission of $SO_2$, and sulphate may increase the emission of ammonia. The costs to deal with these emissions and the additional fly ash produced by sulphur/sulphate addition are not taken into account. There are different ways to prevent emissions, and a cost is difficult to establish. However, to compare addition of sulphur and sulphate, the cost of the additive provides enough information. The price of solid ammonium sulphate is 238$/ton. In the am2 case, about 4.23 kg/h of ammonium sulphate was consumed. The cost is then 1$/h, corresponding to 0.17$/MW h. The price of elemental sulphur is presently 507$/ton. In the 6S case

**Table 5**
The costs of the countermeasures

| Countermeasure | Problem to solve | |
|---|---|---|
| | Agglomeration | Deposits |
| Kaolin | $\leqslant$ 0.43$/MW h | 3.4$/MW h |
| Sulphur | No effect | 0.31 $/MW h |
| Ammonium sulphate | Possible effect | 0.17$/MW h |
| Blast furnace slag | Can be economical | No effect |

3.76 kg/h of sulphur was added. The cost is then 1.9$/h, corresponding to 0.31$/MW h. It should be pointed out that the elemental sulphur gave rise to higher emission of $SO_2$ and that it only brought the concentration of KCl down to 10 ppm; however, without causing KCl to appear in the deposits.

It appears as though kaolin is too expensive to use for this purpose, and that ammonium sulphate is the cheapest and best alternative. The cost of the dosage systems has not been discussed here. In many boilers, addition of kaolin or elemental sulphur can be performed by use of existing equipment. For example, in the present case, the lime supply system was used for kaolin. Even though it may take some adjustments, it does not require large investments. Ammonium sulphate should be supplied as an aqueous solution. This requires a tank, a pump, a spray nozzle and hole in the boiler wall at a suitable place. Usually, such equipment has to be acquired. Therefore, even though ammonium sulphate is more effective and cheaper than sulphur, the latter can be suitable as a first action to address the KCl-induced problems in a boiler.

Table 5 summarizes the costs of the countermeasures that technically can counteract alkali problems.

## 6. Conclusions

Of the methods tested, only addition of kaolin and the use of blast-furnace slag as bed material were found to counteract bed agglomeration. The lowest dosage of kaolin was sufficient and probably it can be even lower. The cost of kaolin addition is around 0.43$/MW h. Blast-furnace slag is economical if the bed regeneration can be decreased to 25% of the corresponding regeneration when silica sand is used. This can probably be done, but kaolin addition appears to be the best method to avoid agglomeration.

Technically, addition of kaolin, ammonium sulphate and elemental sulphur can reduce the flue-gas concentration of KCl to an acceptable level, which leads to little or no deposition of KCl on superheater tubes. However, kaolin is too expensive to be competitive. The efficiency is highest and the cost is lowest for ammonium sulphate.

## Acknowledgements

This project was financed by Värmeforsk AB (project number: A5-509, report number: 997) and by the Swedish Energy Agency. Deposit steel rings were supplied by Sandvik Materials Technology. The project was carried out in cooperation with Solvie Herstad Svärd and Marianne Gyllenhammar (Scandinavian Energy Project) and Håkan Kassman (Vattenfall Power Consultant). The experiments were performed with support from staff at the division of Energy Technology at Chalmers University of Technology and Akademiska Hus AB.

## References

Almark, M., Hiltunen, M., 2005. Alternative bed materials for high alkali fuels. In: Proceedings of the 18th International Conference on Fluidized Bed Combustion. The American Society of Mechanical Engineers, New York. Paper No. 78094.

Baxter, L.L., Miles, T.R., Miles Jr., T.R., Jenkins, B.M., Milne, T., Dayton, D., Bryers, R.W., Oden, L.L., 1998. The behavior of inorganic material in biomass-fired power boilers: field and laboratory experiences. Fuel Processing Technology 54, 47–78.

Broström, M., Kassman, H., Helgesson, A., Berg, M., Andersson, C., Backman, R., Nordin, A., 2007. Sulfation of corrosive alkali chlorides by ammonium sulfate in a biomass fired CFB boiler. Fuel Processing Technology 88, 1171–1177.

Brus, E., Öhman, M., Nordin, A., Broström, D., Hedman, H., Eklund, A., 2004. Bed agglomeration characteristics of biomass fuels using blast-furnace slag as bed material. Energy & Fuels 18, 1187–1193.

Davidsson, K.O., Korsgren, J.G., Pettersson, J.B.C., Jäglid, U., 2002. The effect of fuel washing techniques on alkali release from biomass. Fuel 81, 137–142.

Davidsson, K.O., Steenari, B.-M., Eskilsson, D., 2007a. Kaolin addition during biomass combustion in a 35 MW circulating fluidized-bed boiler. Energy & Fuels 21, 1959–1966.

Davidsson, K.O., Åmand, L.-E., Elled, A.-L., Leckner, B., 2007b. Effect of cofiring coal and biofuel with sewage sludge on alkali problems in a circulating fluidized bed boiler. Energy & Fuels 21, 3180–3188.

Ergudenler, A., Gahly, A.E., 1993. Agglomeration of silica sand in a fluidized bed gasifier operating on straw. Biomass and Bioenergy 4 (2), 135–147.

Hansen, L.A., Nielsen, H.P., Frandsen, F.J., Dam-Johansen, K., Hörlyck, S., Karlsson, A., 2000. Influence of deposit formation on corrosion at a straw-fired boiler. Fuel Processing Technology 64, 189–209.

Iisa, K., Lu, Y., Salmenoja, K., 1999. Sulfation of potassium chloride at combustion conditions. Energy & Fuels 13, 1184–1190.

Kassman, H., Andersson, C., Högberg, J., Åmand, L.-E., Davidsson, K., 2006. Gas phase alkali chlorides and deposits during co-combustion of coal and biomass. In: Winter, F. (Ed.), Proceedings of the 19th FBC Conference, vol. II.

Michelsen, H.P., Frandsen, F., Dam-Johansen, K., Larsen, O.H., 1998. Deposition and high temperature corrosion in a 10 MW straw fired boiler. Fuel Processing Technology 54, 95–108.

Miles, T.R., Miles Jr., T.R., Baxter, L.L., Bryers, R.W., Jenkins, B.M., Oden, L.L., 1996. Boiler deposits from firing biomass fuels. Biomass and Bioenergy 10 (2–3), 125–138.

Nielsen, H.P., Frandsen, F.J., Dam-Johansen, K., Baxter, L.L., 2000. The implications of chlorine-associated corrosion on the operation of biomass-fired boilers. Progress in Energy and Combustion Science 26, 283–298.

Öhman, M., Nordin, A., 2000. The role of kaolin in prevention of bed agglomeration during fluidised bed combustion of biomass fuels. Energy & Fuels 14, 618–624.

Öhman, M., Nordin, A., Skrifvars, B.-J., Backman, R., Hupa, M., 2000. Bed agglomeration characteristics during fluidized bed combustion of biomass fuels. Energy & Fuels 14, 169–178.

Steenari, B.-M., Lindqvist, O., 1998. High-temperature reactions of straw ash and the anti-sintering additives kaolin and dolomite. Biomass and Bioenergy 14 (1), 67–76.

Theis, M., Skrifvars, B.-J., Zevenhoven, M., Hupa, M., Tran, H., 2006. Fouling tendency of ash resulting from burning mixtures of biofuels. Part 2: deposit chemistry. Fuel 85, 1992–2001.

Valmari, T., Lind, M., Kauppinen, E.I., Sfiris, G., Nilsson, K., Maenhaut, W., 1999. Field study on ash behavior during circulating fluidized-bed combustion of biomass. 2. Ash deposition and alkali vapor condensation. Energy & Fuels 13, 390–395.

Werkelin, J., Skrifvars, B.-J., Hupa, M., 2005. Ash-forming elements in four Scandinavian wood species. Part 1: summer harvest. Biomass and Bioenergy 29, 451–466.

Westberg, H.M., Byström, M., Leckner, B., 2003. Distribution of potassium, chlorine, and sulfur between solid and vapor phases during combustion of wood chips and coal. Energy & Fuels 17, 18–28.